DOI https://doi.org/10.5281/zenodo.10049652#114

TWIST, 2024, Vol. 19, Issue 1, pp. 470-480

TWIST

Journal homepage: www.twistjournal.net

Physicochemical Characterization, Thermal Analysis, Biological Studies and Molecular Docking Studies of Cefoperazone Complexes as Anti-Breast Cancer

Essam A. Mohamed
[1]- Department of Chemistry, Faculty of Science, Damanhour University, Egypt
[2]- Department of Chemistry, Faculty of Science and Arts, Sajir, Shaqra University, Kingdom of Saudi Arabia

Alaa E. Ali
Department of Chemistry, Faculty of Science, Damanhour University, Egypt

Sherif A. Kolkaila*
Department of Chemistry, Faculty of Science, Damanhour University, Egypt
[**Corresponding author*]

Mahmoud H. Emara
Department of Chemistry, Institute of Graduate Studies and Environmental Research, Damanhour University, Egypt

Gehan S. Elasala
Department of Chemistry, Faculty of Science, Damanhour University, Egypt

Abstract
The synthesis, physicochemical characterization, and thermal analysis of cefoperazone with transition metals (Cr(III), Mn(II), Fe(III), Co(II), Ni(II), Cu(II), Zn(II), Cd(II), and Hg(II) are investigated. Cefoperazone is found to serve as a bidentate ligand. From magnetic measurements and spectral data, octahedral structures were hypothesized for all complexes except Ni, Cu, and Hg, which possessed tetrahedral structures. TGA and DTA were used to suggest thermal degradation pathways for prepared compounds. The thermal breakdown resulted in the creation of metal oxides and carbon residue as a final product. Molecular docking studies of some complexes as anti-breast cancer.

Keywords
Cefoperazone complexes, Thermal analysis, Molecular docking, Breast cancer

INTRODUCTION

Cephalosporins are categorized into five generations based on their antibacterial activity and evolutionary history. Each newer generation is significantly more active against Gram-negative bacteria than the preceding generation [1]. While the third generation has certain outliers, it has better Gram-negative action against Enterobacteriaceae and less Gram-positive activity. Cephalosporins appear to inhibit bacterial cell wall formation in a way similar to penicillin. Resistance to cephalosporins may be due to the antibiotic's failure to reach its target site. Bacteria can also develop enzymes (betalactamases or cephalosporinases) that can disrupt the betalactam ring, rendering the cephalosporin inert [2]. A third-generation cephalosporin antibiotic known by the brands Cefobid and Cefrone is Cefoperazone Fig. 1. It is among the few cephalosporin medicines that effectively treat infections caused by the Pseudomonas bacteria. With its wide range of action, cefoperazone has been used to combat bacteria that cause infections of the skin, female genital tract, respiratory and urinary tracts, and skin. This article's primary goal is to investigate the biological behavior and complexion characteristics of cefoperazone and its metal complexes. Cefoperazone can create a five-membered ring with metal ions during complex formation, resulting in good stability for the produced complexes. The current study discusses cefoperazone complex preparation, IR, electronic spectra, elemental analysis, magnetic susceptibility tests, thermogravimetric and differential thermal analysis. The mechanism of decomposition is explained, and the thermodynamic parameters are assessed and discussed. Molecular docking studies of cefoperazone metal complexes are discussed.

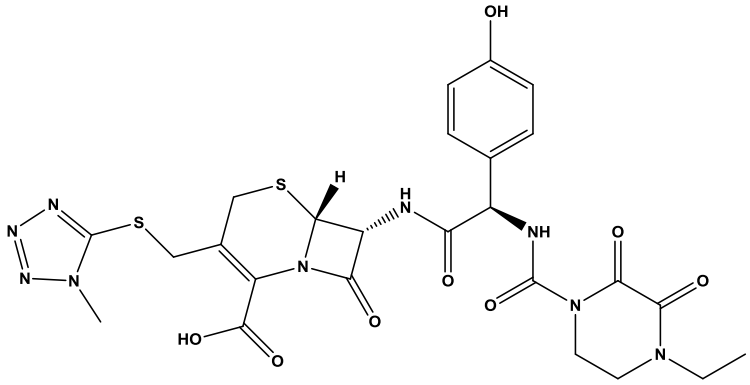

Fig. 1 Structure of Cefoperazone

EXPERIMENTAL

Cefoperazone metal complexes were prepared in a similar manner. The inorganic salts [Cr(III), Mn(II), Fe(III), Co(II), Ni(II), Cu(II), Zn(II), Cd(II) and Hg(II) as metal chlorides] were dissolved in 40 mL bidistilled water. ligand was dissolved in bidistilled water. The molar amount of the metal chloride salt was mixed with the calculated amount of the ligand using different mole ratios (M:L) viz. 1:1. In each case, the reaction mixture was refluxed for about 5 min then left over-night; coloured products precipitated and were isolated by filtration. The products were washed with water and EtOH-H_2O and dried in a vacuum desiccator over anhydrous $CaCl_2$. The analytical studies, Table (1),of all the synthesized complexes were done by the usual methods [3]. The metal contents were determined based on atomic absorption technique using model 6650 Shimadzu-atomic absorption spectrophotometer and complexometrically with standard EDTA solution using the appropriate indicator as reported [4]. The analysis of chloride contents of the complexes were determined by applying the familiar Volhard method [5]. The proposed structures of synthesized metal complexes were illustrated in Fig. 2.

PHYSICAL MEASUREMENTS

The infrared spectra of the cefoperazone and its metal complexes were acquired on potassium bromide disc using a Perkin Elmer spectrophotometer, Model 1430, covering the frequency range of 200-4000 cm^{-1}. Calibration of frequency reading was made with polystyrene film (1602 ± 1 cm^{-1}). The UV–Vis spectra of the solid complexes were measured in Nujol mull spectra [5]. Molar magnetic susceptibilities, corrected for diamagnetism using Pascal's constants were determined at room temperature (298 K) using Faraday's method. The instrument was calibrated with $Hg[Co(SCN)_4]$..Differential thermal analysis (DTA) and thermogravimetric analysis (TGA) of the ligand (cefoperazone) and their complexes were carried out using a Shimadzu DTA/TGA-50. The rate of heating was 20 °C/min. The cell used was platinum and the atmospheric nitrogen rate flow was 20 ml/ min.A molecular docking study was conducted by Molegro virtual docker The 3D structure of the selected protein 3S7S was adopted from the protein data bank As docking initial steps, the protein structure was set up by removing water molecules and adding hydrogen atoms. Also, a site finder was used for the ligand-binding site prediction. Evaluation of the best binding pose between the investigated ligands and the receptor protein was based on the H-bond length and the scoring energy of the simulated docked complex [6].

Table 1 Elemental analysis, stoichiometries and colour of Cefoperazonee complexes

Complexes	Colour	Calculated/(Found)%					
		C	H	N	S	M	Cl
[Cr(cefoperazone)$(OH)_2$(Cl)(H_2O)]	Violet	39.12 (39.95)	4.04 (4.22)	15.79 (14.94)	8.03 (7.70)	6.51 (6.32)	4.44 (4.73)
[Mn (cefoperazone)$_2$Cl(H_2O)]	Yellow	41.36 (41.44)	4.71 (4.42)	17.22 (17.82)	7.89 (7.72)	6.76 (6.37)	4.37 (4.73)
[Fe(cefoperazone)$_2Cl_2$.]	Dark brown	42.42 (42.5)	3.70 (3.72)	17.80 (17.81)	9.06 (9.12)	3.94 (3.97)	5.01 (5.06)
[Co(cefoperzone)$_2$ClH_2O]	Pink	41.74 (41.92)	5.14 (5.51)	16.23 (16.12)	7.43 (7.11)	6.83 (6.13)	4.11 (4.99)
[Ni(cefoperazone) Cl(H_20)]	Indigo	40.41 (40.11)	4.17 (4.16)	16.31 (16.12)	8.30 (8.62)	7.59 (7.60)	4.59 (4.70)
[Cu(cefoperazone) Cl (H_2O)]	Green	38.39 (38.11)	3.74 (3.92)	16.12 (16.77)	8.20 (7.91)	8.14 (8.12)	9.07 (10.23)
[Zn(cefoperazone) Cl (H_2O)]	Yellow	39.33 (39.22)	3.70 (3.41)	16.51 (16.77)	8.40 (8.55)	8.56 (8.44)	4.46 (4.73)
[Cd (Cefoperazone)$_2$Cl (H_2O)]	Yellow	35.72 (35.10)	3.36 (3.45)	16.66 (16.12)	7.37 (7.12)	13.37 (14.73)	4.22 (4.22)
[Hg(Cefoperazone) Cl (H_2O)]	White	33.41 (33.42)	3.14 (3.15)	14.03 (14.01)	7.14 (7.15)	22.32 (22.31)	3.94 (3.95)

All the complexes have m.p > 300º C

RESULTS AND DISCUSSION

The broad bands at 3297.02 –3290.56 cm^{-1} in the systems could be assigned to ν_{O-H} involved in hydrogen bond, due to the presence of coordinated water molecules in all prepared complexes (Table 2) while for [Cu(cefoperazone)Cl(H_2O)] complex, the band at 3428.81 cm^{-1} could be taken as an indication of lattice water. It seems from the elemental analysis of the complexes and thermal analysis that all complexes contain water molecules in their structures. Generally, the ring carbonyl absorption frequency will be shifted to higher wave numbers as the ring becomes more and more strained. The lactam (C=O) band appears at 1770.3 cm^{-1} in the spectrum of cefoperazone which is shifted in the simple complexes spectra (1776.67- 1787.37 cm^{-1}) range. The amide C=O-NH band appears at 1677.80 cm^{-1} in the spectrum of cefoperazone while the complexes show this band at 1674.51- 1675.34 cm^{-1}, suggesting that ligand coordination with these metal ions occurs through the oxygen from the lactam carbonyl group rather than the amide carbonyl group, where the shifting was not significant. The band due to ν_{C-N} of β-lactam ring (1233.23cm^{-1}), and ν_{N-O} of oxime (1011.61 cm^{-1}) in the free ligand remain unchanged on complexation. The band at 1610.09 cm^{-1}, corresponding to the carboxylate asymmetrical stretching of the free ligand is shifted (1- 4 cm^{-1}) to higher wave numbers in the spectra of the complexes indicating coordination through that group [7]. In the far IR spectra, the bonding of nitrogen and oxygen is provided by the presence of bands at 450.37 $cm^{-1}\nu_{(M-N)}$ and 464.22-495.61 $cm^{-1}\nu_{(M-O)}$ [8].

Table 2 Fundamental infrared bands (cm^{-1}) of cefoperazone and its metal complexes

Compound	νNH	ν(C=O) lactam	ν(C=O) amide	ν (COO) asym	ν (COO) sym	ν (C-N) of ß-lactam	ν C-O stretch	νM-N	νM-O	νM-Cl
Cefoperazone	3425	1770	1677	1610	1364	1461	1011	-	-	-
[Cr(cefoperazone)$(OH)_2(Cl)(H_2O)$	3290	1776	1674	1615	1364	1460	1012	534	435	343
[Mn (cefoperazone)$_2$Cl(H_2O)]	3298	1767	1675	1615	1365	1461	1013	524	440	342
[Fe (cefoperazone)$_2Cl_2$.]	3295	1782	1675	1615	1365	1461	1015	523	442	350
[Co(cefoperzone)$_2$Cl(H_2O)]	3392	1776	1676	1615	1365	1462	1011	523	430	360
[Ni(cefoperazone) Cl(H_2O)]	3293	1778	1675	1615	1366	1462	1012	524	432	362
[Cu (cefoperazone) Cl (H2O)]	3428	1758	1657	1614	-	1461	1018	523	450	362
[Zn(cefoperazone)Cl (H_2O)]	3296	1782	1675	1615	1387	1461	1017	491	423	392
[Cd (Cefoperazone)$_2$Cl(H_2O)]	3297	1782	1675	1615	1368	1462	1019	524	427	377
[Hg(Cefoperazone)Cl (H_2O)]	3284	1787	1674	1613	1365	1460	1012	525	422	342

Electronic spectral and magnetic studies

The electronic absorption spectra for all complexes are listed in Table 3 which indicates absorption, transitions of each complex which explain the geometry of each complex. Zn, Hg and Cd complexes exhibited only a high intensity band at 227-244 nm, which are assigned to ligand →metal charge transfer. Owing to the d10- configuration of Zn(II), Cd(II) and Hg(II), no d-d transition could be observed and therefore the strerochemistry around these metals in its complexes can be hardly determined.

Table 3 Nujol mull electronic absorption spectra λ_{max} (nm), room temperature effective magnetic moment values (μ_{eff} 298°K) and geometries of cefoperazone metal complexes

Complex	λ_{max} (nm)	transitions	μ_{eff}	Geometry
[Cr(cefoperazone)$(OH)_2(Cl)(H_2O)$]	278,410, 547	$^4A_{2g}\rightarrow{}^4T_{2g}$ (F), $^4A_{2g}\rightarrow{}^4T_{1g}$(F) $^4A_{2g}\rightarrow{}^4T_{1g}$(p)	3.40	O_h
[Mn (cefoperazone)$_2$Cl(H_2O)]	205.4, 424.8, 446.2, 693.2	$^6A_{1g}\rightarrow{}^4A_{1g}$ $^6A_{1g}\rightarrow{}^4T_{2g}$ $^6A_{1g}\rightarrow{}^4T_{1g}$	4.92	O_h
[Fe(cefoperazone)$_2Cl_2$.]	257, 322,	CT ($t_{2g}\rightarrow\pi^*$) CT ($\pi\rightarrow e_g$)	5.7	O_h
[Co(cefoperzone)$_2$ClH_2O]	301, 426.4, 516.4	$^4T_{1g}$(F) → $^4T_{2g}$(P)	5.85	O_h
[Ni(cefoperazone) Cl$H_2$0]	248.2, 426.2, 638.6	$^3T_1$(F)→$^3T_1$(P), $^3T_1$(F)→$^3A_2$	2.78	T_d
[Cu(cefoperazone)Cl(H_2O)]	254.4, 425	$^2E_g\rightarrow{}^2T_{2g}$ (D)	3.6	T_d
[Zn(cefoperazone)Cl(H_2O)]	227.	ligand→ metal charge transfer	diamagnetic	T_d
[Cd (Cefoperazone)$_2$Cl(H_2O)]	235	ligand→ metal charge transfer	diamagnetic	O_h
[Hg(Cefoperazone)Cl (H_2O)]	244	ligand→ metal charge transfer	diamagnetic	T_d

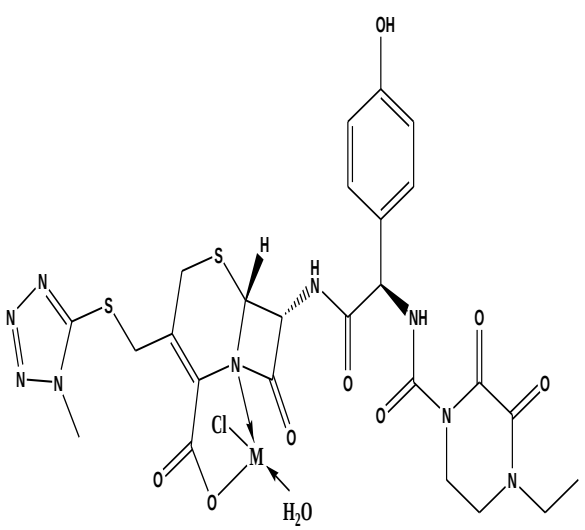

M= Ni ,Cu ,Zn , Hg
[M(cefoperazone) ClH_20]

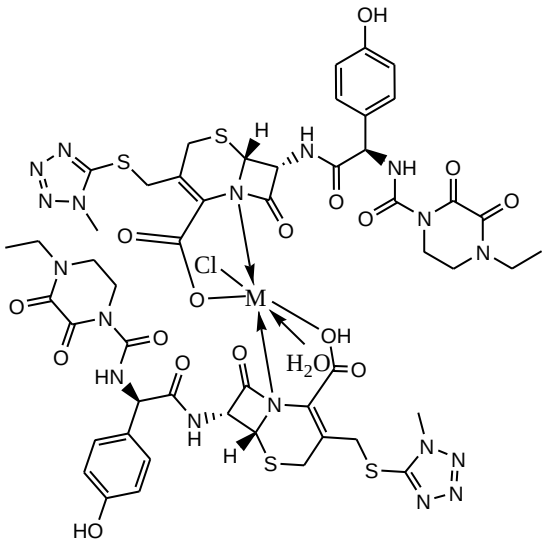

M = Mn ,CO ,Cd
[$M(cefoperazone)_2Cl(H_2O)$]

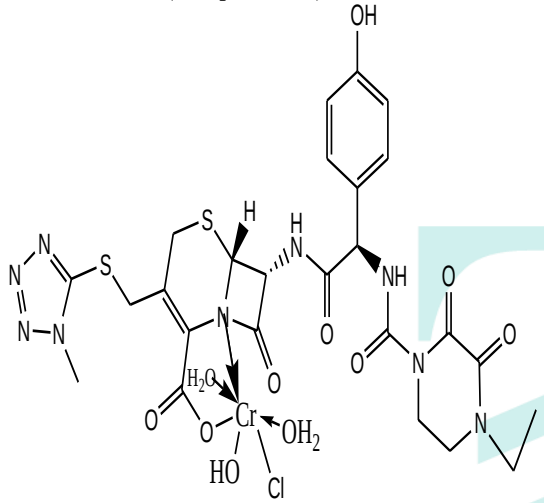

[$Cr(cefoperazone)(OH)\ (Cl)(H_2O)_2$]

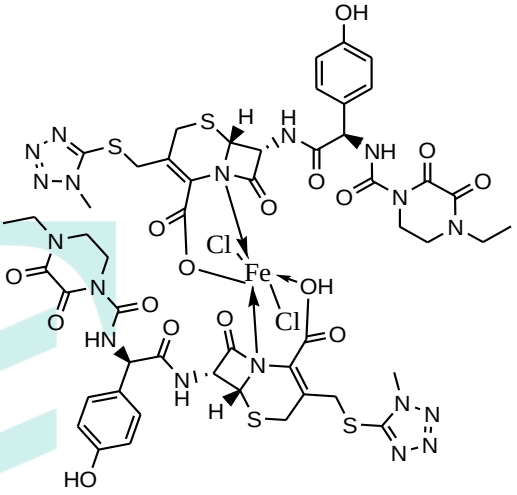

[$Fe(cefoperazone)_2Cl_2$.]

Fig. 2 Proposed structures of cefoperazone complexes

Thermal analysis

The thermal behavior of cefoperazone and it's Zn complex of was investigated by thermograms (TG and DTA), Fig. 3 and the corresponding thermal analysis data is presented in Table 4 [9-16]. In the case of cefoperazone), the decomposition occurs in four exothermic steps 50-600 °C range. There is no mass loss up to 200 °C. The first stage of decomposition starts at 22 °C and ends at 200 °C with a corresponding weight loss 10.1%, Which is accompanied by exothermic effect in the DTA curve. The second stage of decomposition is observed at 201-288 °C (43.43% wt loss). Meanwhile the DTA curve exhibits exothermic effect in the range 210 °C which is accompanied by weight loss confirming. The third stage of decomposition starts at 289 °C and ends at 496 °C with a corresponding weight loss 67.41 % which is accompanied by exothermic effect in the DTA curve. The last stage of decomposition start at 497 °C and ends at 400 °C (94.61% wt loss) Meanwhile the DTA curve exhibits exothermic effect in the range 210 °C which is accompanied by confirmed weight loss.

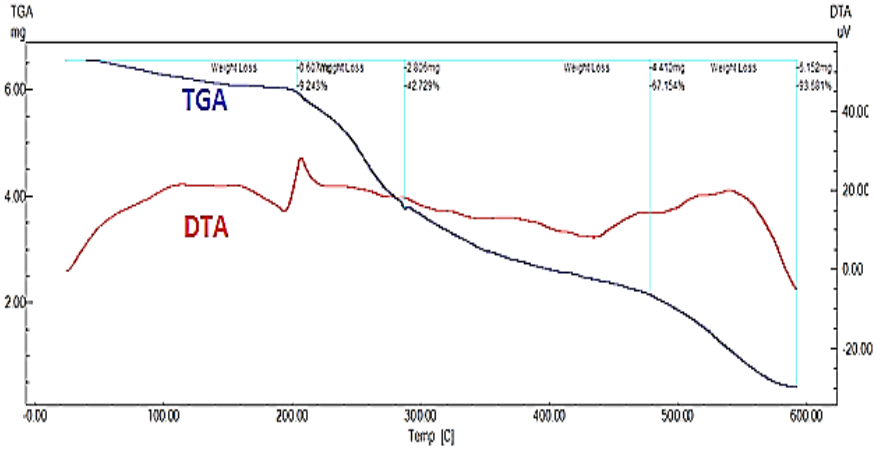

Fig. 4 TGA and DTA of cefoperazone ligand

The suggested mechanism is given as follows:

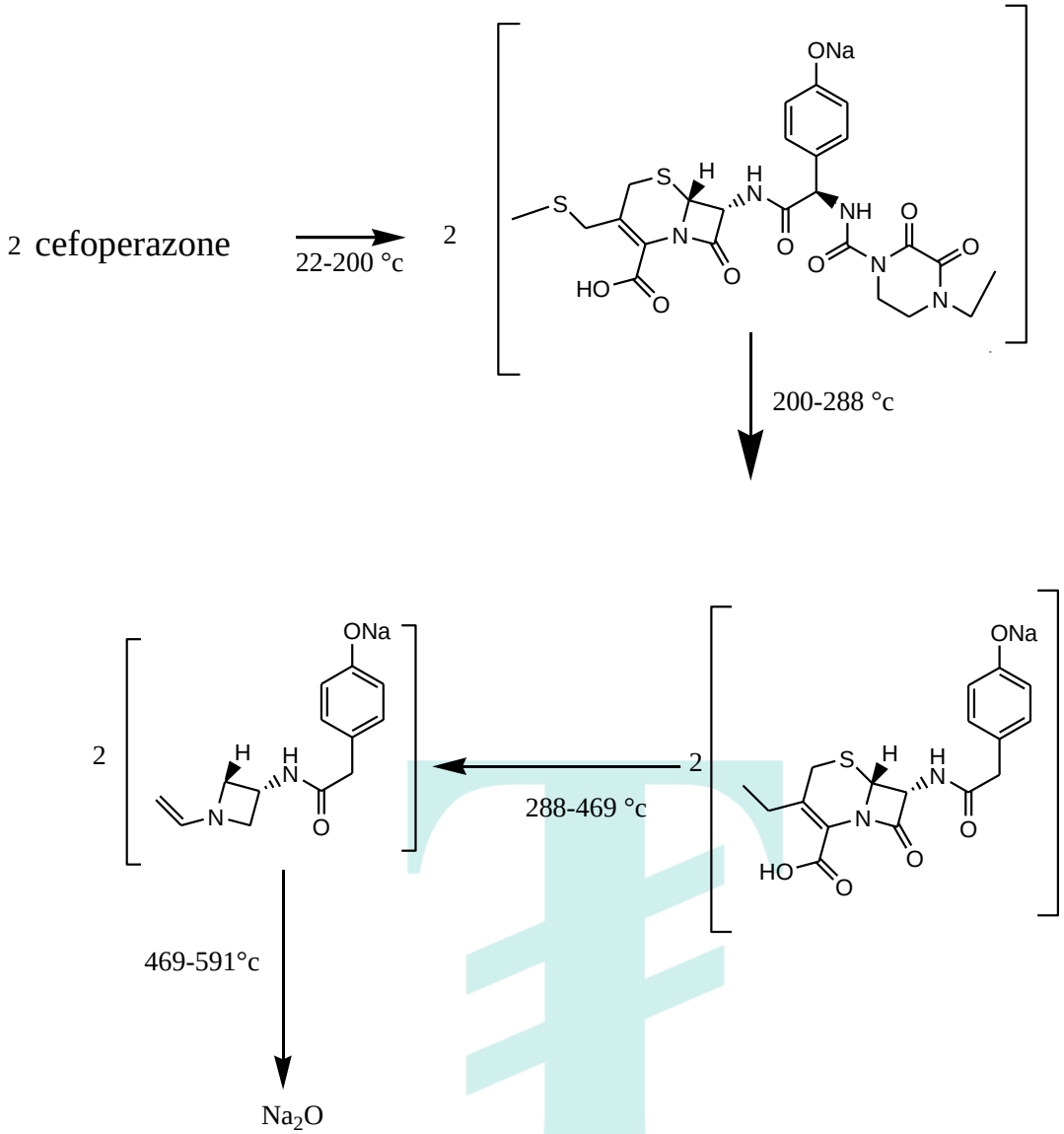

Scheme (1): Themolysis of cefoperazone ligand

In the case of [Zn(cefoperazone)Cl(H_2O)]complex, Fig. 4, the first stage of decomposition starts at 25 °C and ends at 200 °C with a corresponding weight loss 9.39%, which is accompanied by endothermic effect in the DTA curve in the range 123°C which is accompanied by confirmed weight loss. The second stages of decomposition are observed at 280-400 °C (52.36 % wt loss), meanwhile the DTA curve exhibits exothermic effect in the range 260 °C which are accompanied by confirmed weight loss. The last stage of decomposition start at 420 °C and ends at 505 °C (91.78% wt loss) .meanwhile the DTA curve exhibits exothermic effect in the range 471.5 °C which is accompanied by confirmed weight loss.

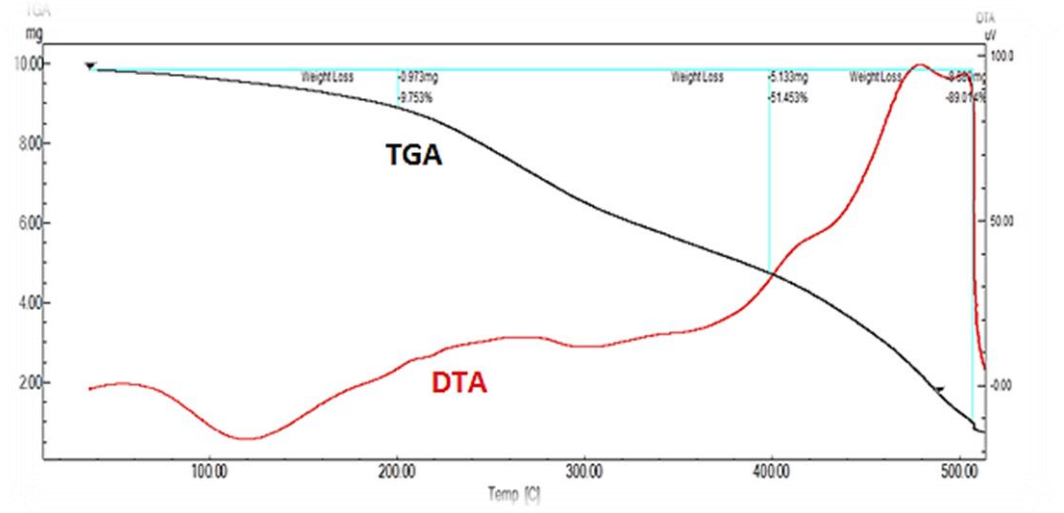

Fig. 5 TGA and DTA of Zn- cefoperazone complex

The suggested mechanism is given as follows:

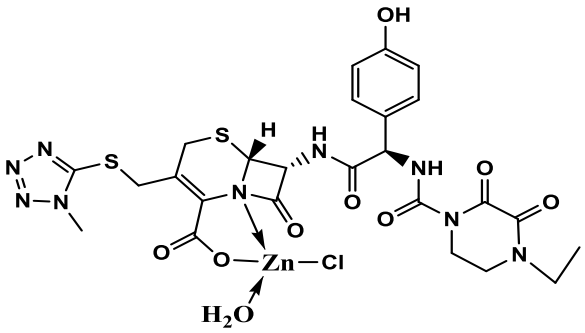

aqua chloro (Cefoperazone)zinc(II)

25-200°C

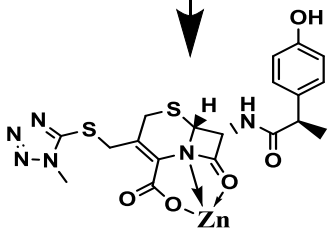

(7-[2-(4-Hydroxy-phenyl)-propionylamino]-3-(1-methyl-1*H*-tetrazol-5-ylsulfanylmethyl)-8-oxo-5-thia-1-aza-bicyclo[4.2.0]oct-2-ene-2-carboxylic acid)zinc(II)

+

280-400°C

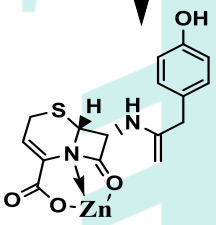

(7-[1-(4-Hydroxy-benzyl)-vinylamino]-8-oxo-5-thia-1-aza-bicyclo[4.2.0]oct-2-ene-2-carboxylic acid)zinc(II)

420-505°C

ZnO

Scheme (2): Thermolysis of [Zn(cefoperazone)Cl (H_2O)] complex

Table 4 DTA analysis of Cefoperazone and its metal complexes

Compound	Type	Tm (°K)	E_a kJ mol^{-1}	n	α_m	$\Delta S^{\#}$ kJ K^{-1} mol^{-1}	$\Delta H^{\#}$ kJ mol^{-1}	Z S^{-1}	Temp. (°C) TGA	Wt. Loss %		Assignment
										Calc	Found	
Cefoperazone	Exo	110	6.34	1.17	0.60	-0.29	-32.6	0.006	22 -200°C	9.24	10.1	loss of $2CHN_4$
	Exo	210	294.49	1.16	0.60	-0.27	-57.9	0.168	200 – 288 °C	42.79	43.34	Loss of $6NH_3$, $4CH_3OH$, 2 CH_3COCH_3
	Exo	377.5	158.77	1.74	0.52	-0.29	-109.7	0.050	288 -496 °C	67.15	67.41	Loss of $6CH_3OH$, $2CH_3SH$,4 NH_3
	Exo	541	47.02	0.94	0.64	-0.30	-166.0	0.010	496- 591 °C	93.68	94.61	Loss of $2NH_3$, 2 CH_3COCH_3, $2C_6H_6$, C_4H_{10} .
$[Cu_2(cefoperazone)_2Cl_4(H2O)_2]$	Endo	122.8	24.04	1.38	0.57	-0.28	-35.36	0.02	34- 202 °C	9.75	9.32	Elimination of $2H_2O$ and 3HCl
	Exo	260	31.68	1.18	0.60	-0.29	-77.48	0.01	202 -430°C	51.63	51.73	Loss of $2C_6H_6O$, $2CHN_4$, $2CH_3COCH_3$, $2CH_3SH$,$2NH_3$and HCl
	Exo	471.5	66.50	1.11	0.61	-0.30	-142.28	0.01	430- 510°C	89.65	89.16	Decomposition of the rest ligand and formation of 2CuO.
$[Zn(cefoperazone)Cl(H_2O)]$	Endo	123	24.04	1.3	0.57	-0.28	-35.36	0.023	25-200 °C	9.75	9.39	Elimination of H_2O,HCl and NH_3
	Exo	260	31.68	1.1	0.60	-0.29	-77.48	0.014	280-400°C	51.45	52.36	Loss of $2NH_3$,$2CH_3COCH_3$, CHN_4 , CH_3OH and CH_3SH
	Exo	471.	66.50	1.1	0.61	-0.30	-142.2	0.016	420-505 °C	89.01	91.78	formation of ZnO

Biological activity

Antibacterial activity

The *in vitro* antimicrobial screening of cefoperazone, and their complexes were performed against the following bacterial strains, *S. pyogenes* , *K. pneumoniae* , *P. mirabilis*, *E. fecalis* , *S. pneumoniae*, *P. aeruginosa*, *E.coli* and *S.aureus* and their efficiency against the bacteria was compared with the standard cefoperazone, Table 5 The minimum inhibitory concentration (MIC) of some selected complexes, which showed significant activity against selected bacterial species, was determined in comparison to the standard antibiotic cefoperazone are summarised in Table 5. The values indicate that the complexes are potentially good inhibitors of the bacterial organisms. It was found that, the chromium complex against *K. pneumoniae*, *P. mirabilis*, *E.coli* and *S.aureus* was found to be having potentially enhanced antibacterial activities as compared to the standard drug. In a broad-spectrum of the bio-potential property, the iron, copper, nickel, zinc complexes were efficient than cefoperazone . among these synthesized complexes, it was found that nickel and copper complexes were more active than cefoperazone against all tested bacteria except *S. pyogenes* and *E. fecalis*. On the other hand, cadmium had similar activty to the standard antibiotic.In general, some metallocefoperzone were found to be enforced potentially with the cefoperazone against the same micro-organisms and under the identical experimental conditions. The increase in efficiency of the metal complexes was due to the participation of metal ion on the demolition of bacterial cell process. The process of complexation reduces the polarity of the metal ion, because of partial sharing of its positive charge with the donor group (ligand) and the electrons delocalized within the metal–ligand complex system. Thus, the complexation favours permeation of the metal through the lipid layers of the microbes'cell membrane. Furthermore, the metal complexes form a hydrogen bond with the active centres of organisms' cell constituents resulting in the perturbation of the normal cell respiratory process of the microbe. Thus, the complexation enhances the penetration and hence the rate of uptake/entrance of the metal into microbial cell and thus able to kill it [(181)].

Also, the higher aggressiveness of zinc (II) complex relative to the rest of the complexes was related to the difference in the effective nuclear charge. During complexation, the decreasing effective nuclear charge (polarity) of the Zn (II) is higher compared to other complexes, which in turn increases the lipophilicity and hence its penetration [17].

Antifungal activity

Antifungal activity of cefoperazone, and their metal complexes were examined against *A. niger*, *A. flavus*, *S. racemosum*, *C. albicans*, *C. glabrata*, *F. oxysporum*, *R. solani* and *A. solani* fungal strains and illustrated in Table 6 and. The minimum inhibitory concentration (MIC) of some selected complexes, which showed significant activity against selected fungi species, was determined in comparison to the standard antibiotic cefoperazone are summarized in Table 6. The values indicate that the complexes are potentially good inhibitors of the fungi organisms. It was found that chromium and nickel complexes exerted significant activity towards *A.flavus*. They were four times (MIC=0.98µg/ml) as active as the standard Amphotericin (MIC=3.9µg/ml), while iron complex showed activity against *A.flavus* two times (MIC=1.95 µg/ml) as active as the reference. On the other hand, mercury complex exhibited activity against *A.niger* four times (MIC=0.12µg/ml) as active as Amphotericin (MIC=0.49µg/ml) and also exerted activity against *A.flavus* sixteen times (MIC=0.24µg/ml) as active as Amphotericin. It was observed that all metallocefoperazone have a promising antifungal activity rather than cefoperazone. The higher activity of the metal complexes may be due to the chelation reduces the polarity of the metal atom mainly because of partial sharing of its positive charge with donor groups and possible electron delocalization over the entire ring. This consequently increases the lipophilic character of the chelates, favoring their permeation through the lipid layers of the bacterial membrane [18-20]

Table 5 The bacterial activity of the free ligands and its complexes against some reference strains expressed in absolute activity (AU)

Compounds	*S. pyogenes* (RCMB010015)	*K. pneumonia* (RCMB001 009)	*P. mirabilis* (RCMB010 085)	*E. fecalis* (RCMB01 0075)	*S. pneumoniae* (RCMB010 029)	*P. aeruginosa* (RCMB01 0043)	*E.coli* (RCMB010 056)	*S.aureus* (RCMB01 0027)
cefoperazone standard	20.6±0.44	16.3±0.19	15.8±0.25	19.6±0.44	20.4±0.44	NA	17.3±0.25	20.3±0.25
[Cr(cefoperazone)$(OH)_2$ $(Cl)(H_2O)$]	18.2±0.58	20.9±0.63	17.2±0.44	16.4±0.63	20.3±0.58	NA	19.6±0.58	20.9±0.63
[Mn $(cefoperazone)_2Cl(H_2O)$]	11.6±0.58	12.9±0.44	NA	NA	14.1±0.44	NA	NA	14.6±0.58
[Fe$(cefoperazone)_2Cl_2$.]	21.3±0.63	22.6±0.63	19.8±0.44	18.4±0.63	21.9±0.37	NA	22.8±0.44	21.9±0.58
[Co$(cefoperzone)_2ClH_2O$]	13.6±0.44	14.5±0.63	NA	NA	15.2±0.63	NA	NA	15.9±0.58
[Ni(cefoperazone) $Cl(H_2O)$]	20.3±0.58	21.2±0.58	18.4±0.63	19.6±0.37	22.9±0.82	18.9±1.2	22.6±0.58	21.4±0.95
[Cu_2(cefoperazone)$_2Cl_4$ $(H_2O)_2$]	20.6±0.58	21.4±0.58	18.6±0.58	17.2±0.63	20.5±0.44	NA	21.3±0.44	21.4±0.58
[Zn(cefoperazone) Cl (H_2O)]	23.5±0.63	25.2±0.14	20.7±0.58	20.1±0.63	24.2±0.44	20.3±0.44	24.5±0.44	23.9±0.58
[Cd (Cefoperazone)$_2$Cl (H_2O)]	20.6±0.44	16.3±0.19	15.8±0.25	19.6±0.44	20.4±0.44	NA	17.3±0.25	20.3±0.25
[Hg(Cefoperazone) Cl (H_2O)]	22.3±0.63	22.99±0.58	19.3±0.44	18.3±0.63	21.9±0.44	NA	21.8±0.63	22.9±0.25

Table 6 Antifungal activity of cefoperazone and their metal complexes

Compounds	*A. niger* (RCMB2317)	*A. flavus* (RCMB02426)	*S. racemosum* (RCMB05922)	*C. albicans* (RCMB05031)	*C. glabrata* (RCMB05274)	*F. oxysporum* (RCMB08213)	*R. solani* (RCMB09421)	*A. solani* (RCMB07324)
Amphotericin B standard	20.4±0.44	17.3±0.25	20.7±0.25	22.0±0.21	21.7±0.58	24.6±0.26	26.7±0.37	24.3±0.44
cefoperazone	11.6±0.44	10.7±0.25	13.2±0.58	NA	11.4±0.37	12.2±0.44	NA	9.4±0.25
[Cr(cefoperazone)$(OH)_2$(Cl) (H_2O)]	18.3±0.44	19.9±0.58	18.0±0.19	NA	16.3±0.44	21.0±0.37	NA	13.0±0.44
[Mn (cefoperazone)$_2$Cl(H_2O)]	13.6±0.44	11.0±0.37	13.4±0.58	NA	12.4±0.58	16.3v0.37	NA	10.4±0.25
[Fe(cefoperazone)$_2Cl_2$.]	19.3±0.44	20.0±0.58	18.2±0.19	NA	16.5±0.44	21.4±0.37	NA	13.7±0.44
[Co(cefoperzone)$_2$ClH_2O]	12.3±0.37	9.3±0.44	10.5±0.58	NA	11.6±0.44	12.4±0.25	NA	10.3±0.44
[Ni(cefoperazone) Cl(H_2O)]	18.2±0.44	19.3±0.58	17.8±0.19	NA	16.3±0.44	20.9±0.37	NA	12.6±0.44
[Cu_2(cefoperazone)$_2Cl_4$ $(H_2O)_2$]	13.3±0.25	12.4±0.44	13.6±0.44	NA	13.7±0.37	15.0±0.37	NA	10.0±0.44
[Zn(cefoperazone) Cl (H_2O)]	13.40.58	12.7±0.37	14.3±0.58	NA	13.8±0.44	17.2±0.25	NA	10.7±0.25
[Cd (Cefoperazone)$_2$Cl (H_2O)]	15.7±0.37	16.1±0.27	13.3±0.44	NA	15.4±0.44	18.3±0.37	NA	11.1±0.25
[Hg(Cefoperazone) Cl (H_2O)]	22.6±0.16	21.9±0.37	19.9±0.28	NA	18.7±0.35	23.4±0.19	NA	15.3±0.12

NA: No activity. The data are expressed in the form of mean± SD

Molecular Modeling of cefoperazone Metal complexes

In the present study, the selected protein 3s7s represents the crystal structure of the human placentalany proposed biologically active compound [21]. This approach elucidates the ligand-receptor site and type of interactions. It also givesan estimation of the distance between the ligand and the receptor inside the interaction grid. The scoring energy of each pose simulated by the docking calculations reflects the degree of inhibition effect of the corresponding ligand. In the present study, the selected protein 3s7s represents the crystal structure of the human placental aromatase enzyme that catalyzes the synthesis of estrogen hormone and contributes to estrogen-dependent breast cancer50. All ligands possess an appreciable extent of interactions with the receptor protein based on the scoring energy . The result show the abibilty of ligand to inhibt 3s7s protien Fig. 6 . The docked (Zn- cefoperazone complex) Fig. 6 have effective ligand-receptor interaction distances were ≤ 3.5 A in most cases, which indicates the presence of typical real bonds and hence high binding affinity . For example, the nearest interaction is observed *via* H-donors with 3S7S (2.40A) and (zn-cefoperaone complex) With mol dock sore 52425 kcal Furthermore, ten binding sites were observed of different amino acids (Ala 438,Trp 141, Arg 435,Arg 145,Arg 115, Cys 437 and phe 438) with zn-cefoperaone complex demonstrating their high inhibition.

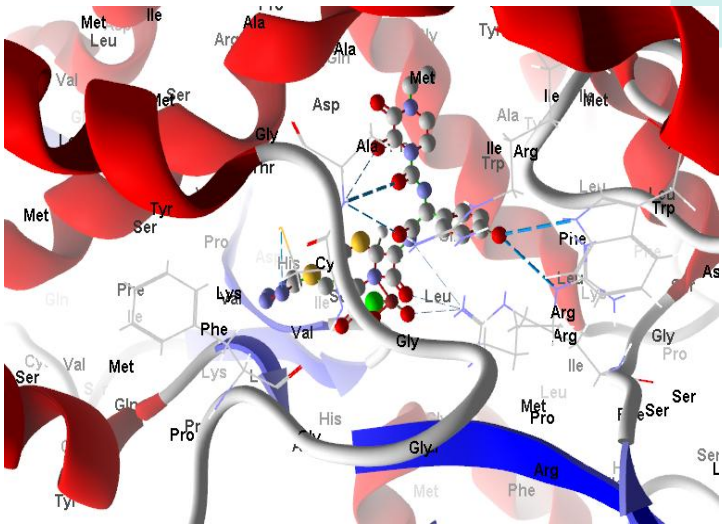

Fig. 6 Virtual Molecular docking of the best docked (zn-cefoperaone complex) with 3s7s

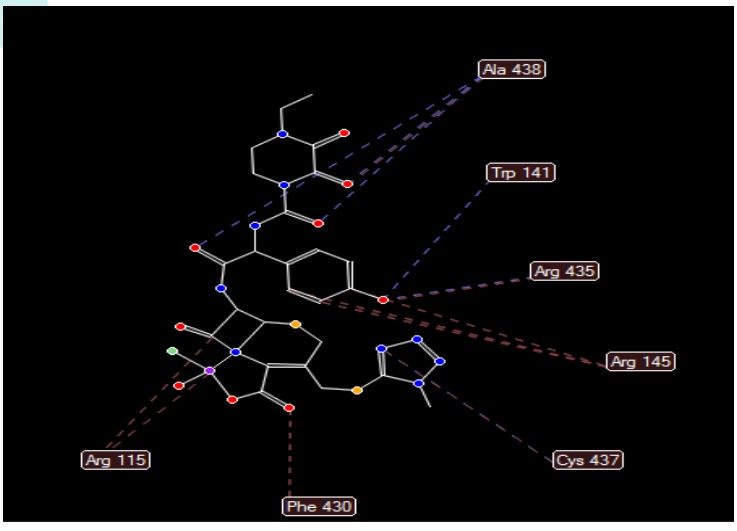

Fig. 7 2D structure of Molecular docking of (complex 2) with 3s7s protein

While the docked (Co-cefoperaone complex) Fig. 8 have effective ligand-receptor interaction distances were ≤ 3.5 A in most cases, which indicates the presence of typical real bonds and hence high binding affinity. For example, the nearest interaction is observed *via* H-donors with 3S7S (2.54A) and (Co-cefoperaone complex) With Mol dock score 46329 kcal Furthermore, ten binding sites were observed of different amino acids(Phe 221 ,Val 370, Met 374, Leu 477, lle 133 and Arg 115) with Co-cefoperaone complex demonstrating their high inhibition.

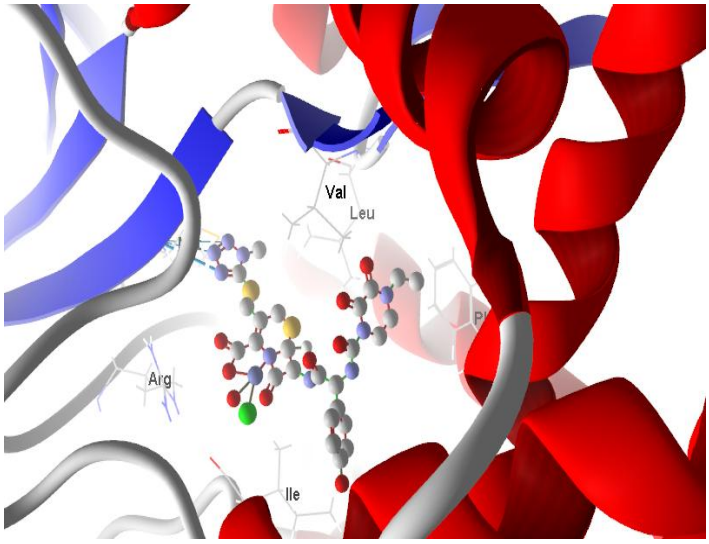

Fig. 8 Virtual Molecular docking of the best docked (Co-cefoperaone complex) with 3s7s

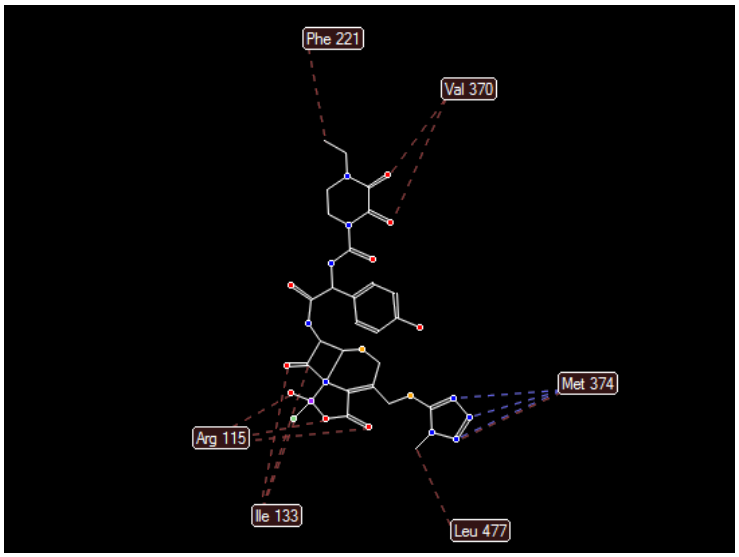

Fig. 9 2D structure of Molecular docking of (Co - cefoperazone) with 3s7s protein

While the docked (Cu-cefoperaone complex) Fig. 10 have effective ligand-receptor interaction distances were ≤ 3.5 A in most cases, which indicates the presence of typical real bonds and hence high binding affinity. For example, the nearest interaction is observed *via* H-donors with 3S7S (2.49A) and (Cu-cefoperaone complex) With Mol dock score 47893 kcal Furthermore, ten binding sites were observed of different amino acids(Ser 478 ,Trp 224, Ala 306,Leu 372, lle 133 and Arg 115) with Cu-cefoperaone complex demonstrating their high inhibition.

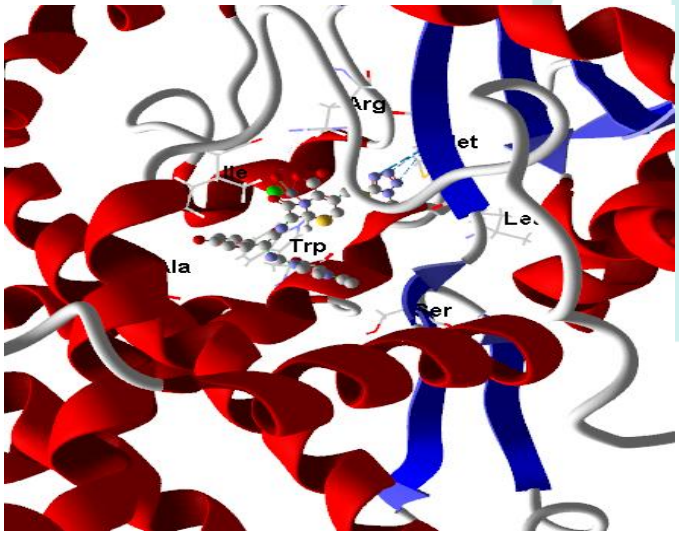

Fig. 10 Virtual Molecular docking of the best docked (Cu-cefoperaone complex) with 3s7s

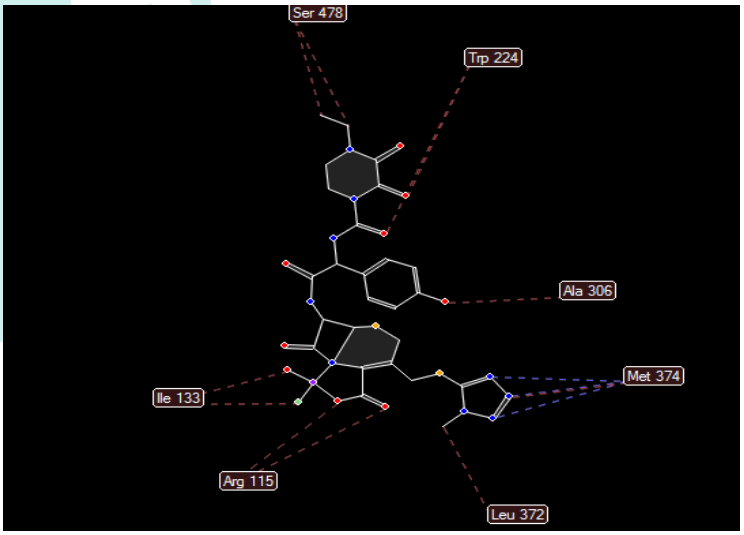

Fig. 11 2D structure of Molecular docking of (Cu - cefoperazone) with 3s7s protein

From the above data it's obtained that Zn > Cu > Co towards inhibition of breast cancer protein 3s7s

CONCLUSION

The synthesis, physicochemical characterization, and thermal analysis of cefoperazone with transition metals (Cr(III), Mn(II), Fe(III), Co(II), Ni(II), Cu(II), Zn(II), Cd(II), and Hg(II) are investigated. Cefoperazone is found to serve as a bidentate ligand. From magnetic measurements and spectral data, octahedral structures were hypothesized for all complexes except Ni, Cu, and Hg, which possessed tetrahedral structures. TGA and DTA were used to suggest thermal degradation pathways for prepared compounds. the thermal breakdown resulted in the creation of metal oxides and carbon residue as a final product. Molecular docking studies of some complexes as anti-breast cancer.

RELEVANT CONFLICTS OF INTEREST/FINANCIAL DISCLOSURES

The authors have declared no conflict of interest. The authors declare that the research was conducted in the absence of any commercial or financial relationships that could be construed as a potential conflict of interest.

REFERENCES

1. Essack S.Y. (2001). The development of β-lactam antibiotics in response to the evolution of β-lactamases. *Pharmaceutical Research*, *18*(10), 1391-1399.
2. Gilman A. G. and Goodman L. S. (1985). The Pharmacological Basis of iSbwapeutics, Macmillan Publishing Company, New York, ch. 50.
3. Vogel A.I. (1989), A Text Book of Quantitative Inorganic Analysis, Longmans, London.
4. Schwarzenbach G. (1957). ‘‘Complexometric Titration’’, Translated by H, Methuen Co., London, Irving.
5. Lee R.H., Griswold E. and Kleinberg J., (1964). Inorg. Chem. 3.
6. Kolkaila S.A. , Ali A.E. and Elasala G.S. (2021). Synthesis, Spectral Characterization of Azithromycin with Transition Metals and a Molecular Approach for Azithromycin with Zinc for COVID-19. *Int J Cur Res Rev.*, *13*, 23, 53-59.
7. Masoud M.S., Ali A.E., Elasala G.S. & Kolkaila S.A. (2018). Synthesis, spectroscopic, biological activity and thermal characterization of ceftazidime with transition metals. *Spectrochim Acta*, *193*, 458-466.
8. Ali A. E. , Elasala G. S., Mohamed E. A. and kolkaila S.A.(2019), Spectral, thermal studies and biological activity of pyrazinamide complexes. *Heliyon*, *5*(11).
9. Ali A.E., Elasala G.S., Mohamed E. A. and kolkaila S.A. (2021). Structural and thermal analysis of some imipramine complexes. J. materials today proceeding.
10. Masoud M.S., Ali A.E., Elasala G.S. and kolkaila S.A. (2017), Synthesis, Spectroscopic Studies and Thermal Analysis on Cefoperazone Metal Complexes. *J. Chem. Pharm. Res*., *9*(4), 171-179.
11. Masoud M.S., Ali A.E., Elasala S. G., S.F sakr, kolkaila S.A(2020),Structural, Physicochemical Studies of Some Biologically Active Metal Complexes of Cefazolin Antibiotics. *J. Chem. Pharm. Res*., *12*, 42-52.
12. Kolkaila S.A. , Ali A.E.,Doha Beltagy and Elasala G.S. (2018), Spectral and Biological Studies of Some Selected Thiouracil, Barbital and Thiobarbituric Acid Complexes. *J Drug Des.Res*., *5*, 2, 1071-1079.
13. Ali A. E.Elmelegy E. , Kolkaila S. A., Mustafa A. A., Eledkawy A. M. and Alnaggar G. A.(2022) Removal of Cadmium (II) from Water by Adsorption on Natural Compound. *Journal of Environmental Treatment Techniques*, *10*(2) 164-169.
14. Kolkaila S.A., Ali A.E. , Mustafa Ahmed A.(2023) Removal of Aluminum (III) from Water by Adsorption on the Surface of Natural Compound. *J. of Environmental Treatment Techniques*, *11*(2) 10-105.
15. Ali A.E., Elasala G.S., Rana M.Atta. and kolkaila S.A.(2022), Synthesis, Thermal Analysis and Characterization of Doxycycline Metal Complexes. *Chemistry Research Journal*, *7*, 2, 90-91.
16. Ali A. E., Elasala G. S., Eldeeb M. H., kolkaila S. A. (2023) Synthesis and Biological Activity and Thermal Analysis of Sulfaquinoxaline Mixed Metal Complexes. *Journal of Chemistry & its Applications*. SRC/JCIA-119.DOI: doi.org/10.47363/JCIA/2023(2)119
17. El-Tabl, A. S., El-Wahed, M. M. A. ., El Kadi, N. M., Kolkaila, S. A., & Samy, M. (2023). Novel Metal Complexes of Bioactive Amide Ligands as New Potential Antibreast Cancer Agents. *TWIST*, *18*(4), 151-169.
18. El-Tabl, A. S., Kolkaila, S. A., Abdullah, S. M., & Ashour, A. M. (2023). Nano-Organometallic Compounds as Prospective Metal BasedAnti-Lung Cancer Drugs: Biochemical and Molecular Docking Studies. *TWIST*, *18*(4), 141-150.
19. El-Tabl, A. S., Dawood , A. A. E. R. ., Kolkaila , S.A., Mohamed , E. H., & Ashour, A. (2023). The Cytotoxicity of Some Biologically Active Nano Compounds against Colon Cancer: Advanced Biochemical Analyses. *TWIST*, *18*(4), 360-371.
20. El-Tabl, A. S., Abd El-Wahed, M. M., Kolkaila, S. A., Abd El-Nasser, A. G., & Ashour, A. M. (2024). Biochemical Studies on Some Novel Organometallic Complexes as Anti-Human Prostate Cancer. *TWIST*, *19*(1), 16-26.
21. Mohamed, E. A., Ali, A. E., Kolkaila, S. A., Fyala, S. S., & Elasala, G. S. (2024). Synthesis, Spectroscopic Studies, Thermal Analysis and Molecular Docking of Chloramphenicol Metal Complexes as Anti-Prostate Cancer. *TWIST*, *19*(1), 400-408